Microvascular Structure Segmentation in Human Tissue Using Deep Learning

MSc Research Project
Data Analytics

Sarvochch Balwant Singh
Student ID: 22163891

School of Computing
National College of Ireland

Supervisor: Prof. Noel Cosgrave

National College of Ireland
Project Submission Sheet
School of Computing

Student Name:	Sarvochch Balwant Singh
Student ID:	22163891
Programme:	Data Analytics
Year:	2023
Module:	MSc Research Project
Supervisor:	Prof. Noel Cosgrave
Submission Due Date:	14/12/2023
Project Title:	Microvascular Structure Segmentation in Human Tissue Using Deep Learning
Word Count:	3378
Page Count:	18

I hereby certify that the information contained in this (my submission) is information pertaining to research I conducted for this project. All information other than my own contribution will be fully referenced and listed in the relevant bibliography section at the rear of the project.

ALL internet material must be referenced in the bibliography section. Students are required to use the Referencing Standard specified in the report template. To use other author's written or electronic work is illegal (plagiarism) and may result in disciplinary action.

Signature:	
Date:	14th December 2023

PLEASE READ THE FOLLOWING INSTRUCTIONS AND CHECKLIST:

Attach a completed copy of this sheet to each project (including multiple copies).	☐
Attach a Moodle submission receipt of the online project submission, to each project (including multiple copies).	☐
You must ensure that you retain a HARD COPY of the project, both for your own reference and in case a project is lost or mislaid. It is not sufficient to keep a copy on computer.	☐

Assignments that are submitted to the Programme Coordinator office must be placed into the assignment box located outside the office.

Office Use Only	
Signature:	
Date:	
Penalty Applied (if applicable):	

Microvascular Structure Segmentation in Human Tissue Using Deep Learning

Sarvochch Balwant Singh
22163891

Abstract

The main objective of this research was to investigate the effective ways in which a 2D photo of a healthy human tissue can be segmented to find blood vessel present in them. Two models were selected for the task first being DeeplabV3+ and the second model U-Net.

After conducting a through research it was evident that both the models had potential for image segmentation in the filed of medical. However U-Net showed a Superior performance compared to DeeplabV3+ it had a better dice coefficient score of 0.68 ± 0.1. The study also showed light on the architecture of Deeplabv3+, however being good in the field of medical image segmentation its complex architecture does not work properly when it comes to identify small details present in the image so it may not be accepted across other medical imaging applications.

This study sheds light on how deep learning models can help professionals in filed of medical by improving healthcare imaging, which is very essential for fast and effective diagnosis. The study also shows some limitations such as the models may perform badly given on the dataset/images that they are provided with.

1 Introduction

Advancements in technological field has changed medical imaging in this fast evolving field, enhancing diagnostic precision and treatment planning. Of all the applications, one of the most important ones is the segmentation of medical pictures, especially the ones that show complex anatomical features. Precisely defining areas of interest, such tumors or blood arteries, is essential for efficient illness diagnosis, tracking, and therapy assessment. In this matter, deep learning techniques paired with image segmentation have shown a lot of promise, offering previously not so heard levels of accuracy and efficiency. The present study starts with an in-depth review of the developments in medical picture segmentation with a particular focus on the use of new and inovative deep learning architectures. The main objective is to look into, evaluate, and compile the results of current studies that use deep learning to segment various anatomical systems. This research attempts to explore the challenges, issues, and breakthrough possibilities of deep learning in medical picture segmentation through a thorough examination of the literature and real-world application.

1.1 Research Question

What methods can be used by machine learning models and image processing technologies to best segment microvascular characteristics in 2D pictures of human tissue that are healthy, such as blood vessels?
The main objective is to carry out a research that makes use of machine learning and image processing methods which will help us segment healthy human tissues and Which deep learning models are most suited for the microvascular segmentation task? An important part will be to look at well-known models such as U-Net, Mask R-CNN, and their variations in the context of segmenting healthy tissue microvasculature.

2 Related Work

Research on the relationship between medical imaging and machine learning has significantly increased in the last several years, especially in the area of tissue segmentation. The purpose of this review of the literature is to summarize and contrast three innovative research that use distinct machine learning techniques for tissue segmentation in diverse medical settings.

2.1 Organ Vascular Segmentation Using Deep Learning

Todorov et al. (2020) describes, a deep learning-based system for segmenting the whole mouse brain vasculature using a convolutional neural network (CNN) with transfer learning is presented: the VesSAP tool. The brain vasculature may be accurately quantified and analyzed by the researchers by combining tissue transparency methods with artificial intelligence. A reference map is provided for different mouse strains using the method, the research sheds light on brain vascular system. Anomalies in brain's blood flow can be detected with the help of this instrument. Takahashi et al. (2022) proposed a the CUBIC technique—which combines topological data analysis with tissue-clearing technology—is introduced for 3D imaging of vascular systems particular to individual organs. Using data analysis and machine learning classification the changes in the mice illness is detected which is carried out effectively. Similar to the Todorov et al. (2020), Todorov et al. (2019) introduces the VesSAP tool and reiterates the importance of comprehending brain vasculature. The tools scalability and not so partial measurement is shown by the researcher when talking about a reference map for the vasculature, when the mouse's brain is transparent and with the use of HD imaging. The researcher has also shed light on how the tool can be used for automated analysis of brain conditions like stoke and Alzheimer's disease.
The work of Oskal et al. (2019) focuses on dermatology, suggests a U-net-based approach for distinguishing epidermal tissue in histological pictures. The researcher makes a strong point on use of CAD to be used for effective diagnosis of skin diseases.After being trained on a large dataset, the U-net model performs better than previous methods and shows resilience to changes in tissue thickness and staining. Kemnitz et al. (2020) discusses osteoarthritic knee discomfort and presents a novel technique for separating adipose tissue from thigh muscle. Clinical assessments may benefit from the suggested U-net-based architecture's efficacy in segmenting tissues related to osteoarthritic knee discomfort.
Wu et al. (2019)'s study, a 2D U-net powered by a 3D fully convolutional neural network is used to simultaneously classify tissues and segment the ventricles. While not

fully explained the technique suggests that combining the models created for 2D and 3D segmentation may provide better results if they are combined together, which is a very unique direction for future research work. The importance of automated liver segmentation in the diagnosis of liver disorders is discussed in Tang et al. (2020)'s article. To achieve precise segmentation without the need for human feature extraction, the authors suggest a two-stage method that combines DeepLab and Faster R-CNN.

Despite the fact that each work significantly advances the field of tissue segmentation, their approaches and areas of concentration differ noticeably. The three research on the brain vasculature (Todorov et al. (2020), Takahashi et al. (2022), and Todorov et al. (2019)) employ machine learning to segment data and provide tools for in-depth examination. However, Oskal et al. (2019), Kemnitz et al. (2020), and Tang et al. (2020) demonstrate the adaptability of machine learning applications by delving into tissue segmentation in various medical scenarios. The use of deep learning models—more especially, CNNs and U-net architectures—to show how successful they are at precise segmentation is a strength shared by all the publications. Moreover, the advancement of medical imaging research is demonstrated by the incorporation of advanced methods such as tissue transparency, topological data processing, and simultaneous 2D-3D modeling.

There still mays some issues persist with different dataset when it comes to standardization and validation. Despite the fact that each study demonstrates efficacy in its particular setting, a uniform criteria is still required to evaluate segmentation strategies and ensure generalizability. Subsequent investigations ought to concentrate on the comprehensibility of these complex models and the integration of multi-modal data to achieve more thorough segmentation.

In summary, these research demonstrate how machine learning has the potential to revolutionize tissue segmentation in a variety of medical fields. The wider use of these novel approaches in clinical practice will depend on how well the field handles standards issues and improves model interpretability.

2.2 Applications of Deep Learning in Tissue Segmentation

Singh and Cirrone (2022) Provides a data-efficient deep learning system for the segmentation and classification of histological images, with a specific focus on samples of dermatomyositis.In case of auto immune diseases the proposed methodology improves classification efficiency and segmentation efficiency but the author also addresses the need for smart and efficient tools that can study the complex structure. Luke et al. (2019) presents the convolutional neural network O-Net, designed for quantitative photoacoustic image segmentation and oximetry. The finding includes a very accurate method of determining the blood's oxygen content at any given time. Through a combination of computer learning and "photoacoustic imaging," the author was able to obtain a far better understanding of blood oxygen levels. Alsenan et al. (2021) uses a deep learning model based on UNet and MobileNetV3 to try and segment the spinal cord's gray matter. The combination of UNet and MobileNetV3 suggests a novel approach for spinal cord gray matter segmentation, albeit specific advantages are not indicated.

The results of 408 investigations on the automated segmentation of organs and tissues using CT and MRI are included in Lenchik et al. (2019) review. The author highlights how can the fast advances on monitoring therapy responses and disease diagnosis can have a positive influence. Wolny et al. (2020) presents PlantSeg, a pipeline for 3D segmentation of plant tissues at cellular resolution that is based on convolutional neural networks.

According to the author a flexible approach will be provided by the proposed tool, that will work better on different kind of tissues, sizes and image condition when it comes to plant biology. A big contribution has been made by this research in regards to the study of plat tissue.

Abdani et al. (2020) focuses on the artificial segmentation of pterygium tissues and uses a deep learning technology in its approach. Keeping efficiency of segmentation in mind author added deeply connected layers to the model. A online screening tool that can be used by the users to detect the diseases was also proposed by the author. Oskal et al. (2019)identifies malignant melanoma by offering a U-net based technique for segmenting epidermal tissue in histopathology images. The suggested method exhibits resilience against changes in tissue properties and staining when incorporated into a computer-aided diagnostic system.

All the studies reviewed make a distinct contribution to medical imaging segmentaiton. Notable for their contributions to the diagnosis of intricate disorders are the histopathology image segmentation framework and the photoacoustic image segmentation network. A comprehensive picture of automatic segmentation across several imaging modalities is offered by the systematic review. PlantSeg uses machine learning to the study of plant biology, whilst the pterygium tissue segmentation and epidermal tissue segmentation articles offer specific solutions for issues with visual manifestations. However, there is a need for more research because the spinal cord gray matter segmentation report is not detailed enough.

2.3 Model-Centric Innovations in Vascular and Tumor Segmentation

The study of Groves et al. (2020) presents the Mask R-CNN and U-Net algorithms and shows how well they work for automated segmentation of the internal jugular vein and carotid artery in the neck vasculature. The vascular reconstruction and its validity with the CT images with the help of Mask R-CNN shows its ability to perform 3D analysis and its significant mark on understanding of vascular structure. Jeong et al. (2020) introduces a novel 3D Mask R-CNN method for brain tumor segmentation in the field of neuroimaging. A more thorough examination is ensured by including dynamic susceptibility contrast-enhanced MRI perfusion pictures. The strong performance measures, such as recall, accuracy, and Dice similarity, highlight its usefulness for tracking disease development and planning radiation treatments. Jahnavi and Vasundhara (2022)'s research presents U-Net++, a thoroughly trained encoder-decoder network with interconnected skip routes, with a focus on retinal arteries. Skip links are carefully designed to reduce semantic gaps and improve retinal vascular recognition accuracy. This novel method may lead to improved diagnosis of age-related macular degeneration, glaucoma, hypertension, and diabetic retinopathy.

Chen et al. (2021) presents DC-U-Net, a fusion of U-Net and dilated convolution, to address the crucial challenge of lung CT image segmentation. Evaluations in comparison to Otsu and area growth algorithms show better results in terms of Dice coefficient and Intersection over Union (IOU). This technique offers improved accuracy for later analysis of lung structures and speeds up segmentation. Mittal et al. (2019)'s study adopts a comprehensive strategy for brain tumor segmentation, including preprocessing, a stacked auto-encoder network for feature extraction, and post-processing morphological filtering. The suggested approach shows improved precision in separating brain cancers from various MRI images. It is a major step forward in addressing low contrast imaging and morphological uncertainty problems.

Saeedizadeh et al. (2021) presents the TV-Unet model for segmenting COVID-19 contaminated areas in chest CT images in response to the worldwide health issue. Its novel addition of a 2D-anisotropic total-variation regularization term enhances segmentation accuracy and makes it a quick and efficient replacement for COVID-19 infection detection. The model's high Dice score and mIoU rate highlight its efficacy. In order to segment brain tumors, Chahal et al. (2019) presents a deep learning model that combines the Two-Pathway and Cascade architectures. The model performs exceptionally well in predicting tumor cells by utilizing convolutional neural networks, which helps it overcome obstacles like low contrast imaging and position ambiguity. The suggested approach shows promising results in automating this difficult process, adding to the larger field of brain tumor segmentation.

Even though every research focuses on different difficulties with medical picture segmentation, they all use deep learning architectures, which highlights how reliable and flexible these methods are. Notably, new designs like DC-U-Net, TV-Unet, and U-Net++ demonstrate continuous attempts to improve segmentation accuracy.

There are, however, a few gaps in the publications. There is still need for progress in areas like the requirement for bigger and more varied datasets, addressing the interpretability of deep learning models, and guaranteeing generalizability to a range of clinical circumstances. Standardization of comparison techniques and performance indicators would also make it easier to conduct a more thorough assessment of various approaches.

3 Methodology

Using a comprehensive study , deep learning models have been applied to the task of medical image segmentation. The method is founded on a scientific process that comprises collecting data, building models, and evaluating them. This work makes use of the Knowledge Discovery in Databases (KDD) method, a systematic approach for extracting useful knowledge from vast volumes of data.

The following figure Figure 1 will give a brief idea about the workflow of the research.

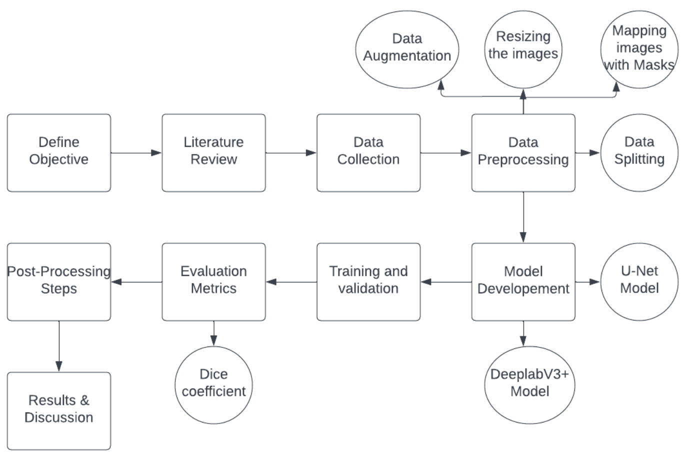

Figure 1: Work Flow of the Research

3.1 Data Collection

The HubMap competition on Kaggle yielded the dataset "HubMap - Hacking the Human Vasculature." High-resolution microscopy pictures of human tissue, with a particular emphasis on the vasculature, are included in this collection. Metadata was gathered that included specifics about picture tiles and full-slide photos. For the segmentation of vascular structures, ground truth annotations—which are essential for supervised training—were accessible. Annotations were provided in the datasets were co-ordinates for each anootation types were provided in a json file. preprocessing techniques were applied to the photos to assure uniform proportions and highlight relevant features. Rotation and flipping were two of the approaches used to improve the training dataset.

3.2 Model Development

During the model selection process, important findings from pertinent research articles using architectures like Deeplabv3 and U-Net were taken into account.

Two popular deep learning architectures were selected for testing: U-Net and DeeplabV3+. Similar medical picture segmentation tests have shown these models to be successful.
U-Net a type of CNN was created for the segmentation of medical images. Its architecture is encoder-decoder. The decoder uses transposed convolutions to achieve exact localization, while the encoder records the image's context. The skip connections between the encoder and the decoder, which aid in retrieving the fine-grained data lost during downsampling, are one of U-Net's primary characteristics Huang et al. (2020).
An expansion of the DeepLabv3 model made for segmentation is called DeepLabV3+. To capture multi-scale context, it provides a module called Atrous Spatial Pyramid Pooling (ASPP) and employs an encoder-decoder structure. In addition, depthwise separable convolution is a feature of DeepLabV3+ that considerably minimizes computation and model size when compared to conventional convolutions Azad et al. (2022).
Medical image segmentation has seen the effective use of both U-Net and DeepLabV3+15. They can preserve high spatial information and capture multi-scale characteristics, both of which are essential for medical picture segmentation.
The models were trained using a training-validation split on the HubMap dataset. To keep an eye on model stability and avoid overfitting, hyperparameters were adjusted iteratively and validation was done on a frequent basis during the training phase.

3.3 Evaluation Methodology

The Dice coefficient, which calculates the overlap between the ground truth and anticipated masks, is the main evaluation measure used.The Dice Coefficient, which is often referred to as the Sørensen-Dice coefficient, is a widely used statistic in the medical imaging industry for assessing image segmentation tasks. In order to compare an expected segmentation mask (also known as an anticipated mask) with the ground truth mask, it estimates the overlap between two binary pictures. The measurements of accuracy and loss are extra. These requirements relate to recognized benchmarks in the field of medical picture segmentation studies. Dice coefficient is defined as -

$$\text{Dice} = \frac{2 \cdot |A \cap B|}{|A| + |B|}$$

where $|A| + |B|$ is the total number of pixels in both the predicted and ground truth masks, and $|A \cap B|$ denotes the common elements (i.e., the properly predicted pixels) between sets A and B.
Choosing evaluation metric also depends upon the dataset and the task that is been carried out,the other options that was present was Intersection over Union (IOU).

3.4 Result Assessment

Via the use of ground truth masks and real photos with predicted masks, the outcomes were qualitatively evaluated. A proper examination of the segmentation quality was done by this qualitative analysis.
Accuracy of segmentation was obtained by calculating quantitative indicators, such as the average Dice coefficient. This method is mostly used in the field of image segmentation.

4 Implementation

Entering the implementation phase is essentially the realization of the research objectives and concepts. Consider it as converting the beliefs and techniques into actual, observable outcomes.

4.1 Data Loading And Visualization

The process starts by loading the necessary libraries and metadata, such as the WSI (Whole Slide Image) and tile metadata. In addition to verifying the quantity of instances available for training and testing, it creates the pathways to the training and test datasets. In order to gain understanding of the dataset's demographic distribution, an exploratory data analysis is carried out.

The annotations are taken from a JSON Lines file called polygons.jsonl, which has the necessary data on the areas of the photos that have been annotated. Figure 2 demonstrates how the annotations and coordinates are present in the Json file

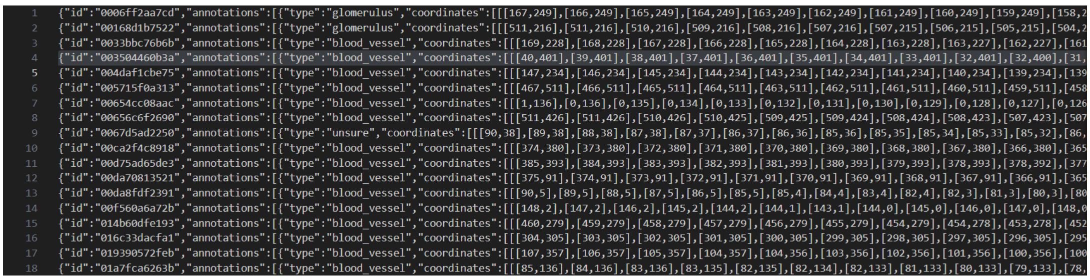

```
{"id":"0006ff2aa7cd","annotations":[{"type":"glomerulus","coordinates":[[[167,249],[166,249],[165,249],[164,249],[163,249],[162,249],[161,249],[160,249],[159,249],[158,2
{"id":"00168d1b7522","annotations":[{"type":"glomerulus","coordinates":[[[511,216],[511,216],[510,216],[509,216],[508,216],[507,216],[507,215],[506,215],[505,215],[504,2
{"id":"0033bbc76b6b","annotations":[{"type":"blood_vessel","coordinates":[[[169,228],[168,228],[167,228],[166,228],[165,228],[164,228],[163,228],[163,227],[162,227],[161
{"id":"003504460b3a","annotations":[{"type":"blood_vessel","coordinates":[[[40,401],[39,401],[38,401],[37,401],[36,401],[35,401],[34,401],[33,401],[32,401],[32,400],[31,
{"id":"004daf1cbe75","annotations":[{"type":"blood_vessel","coordinates":[[[147,234],[146,234],[145,234],[144,234],[143,234],[142,234],[141,234],[140,234],[139,234],[139
{"id":"005715f0a313","annotations":[{"type":"blood_vessel","coordinates":[[[467,511],[466,511],[465,511],[464,511],[463,511],[462,511],[461,511],[460,511],[459,511],[458
{"id":"00654cc08aac","annotations":[{"type":"blood_vessel","coordinates":[[[1,136],[0,136],[0,135],[0,134],[0,133],[0,132],[0,131],[0,130],[0,129],[0,128],[0,127],[0,126
{"id":"00656c6f2690","annotations":[{"type":"blood_vessel","coordinates":[[[511,426],[511,426],[510,426],[510,425],[509,425],[509,424],[508,424],[508,423],[507,423],[507
{"id":"0067d5ad2250","annotations":[{"type":"unsure","coordinates":[[[90,38],[89,38],[88,38],[87,38],[87,37],[86,37],[86,36],[85,36],[85,35],[85,34],[85,33],[85,32],[86,
{"id":"00ca2f4c8918","annotations":[{"type":"blood_vessel","coordinates":[[[374,380],[373,380],[372,380],[371,380],[370,380],[369,380],[368,380],[367,380],[366,380],[365
{"id":"00d75ad65de3","annotations":[{"type":"blood_vessel","coordinates":[[[385,393],[384,393],[383,393],[382,393],[381,393],[380,393],[379,393],[378,393],[378,392],[377
{"id":"00da70813521","annotations":[{"type":"blood_vessel","coordinates":[[[375,91],[374,91],[373,91],[372,91],[371,91],[370,91],[369,91],[368,91],[367,91],[366,91],[365
{"id":"00da8fdf2391","annotations":[{"type":"blood_vessel","coordinates":[[[90,5],[89,5],[88,5],[87,5],[86,5],[85,5],[85,4],[84,4],[83,4],[82,4],[82,3],[81,3],[80,3],[80
{"id":"00f560a6a72b","annotations":[{"type":"blood_vessel","coordinates":[[[148,2],[147,2],[146,2],[145,2],[144,2],[144,1],[143,1],[144,0],[145,0],[146,0],[147,0],[148,0
{"id":"014b60dfe193","annotations":[{"type":"blood_vessel","coordinates":[[[460,279],[459,279],[458,279],[457,279],[456,279],[455,279],[454,279],[454,278],[453,278],[452
{"id":"016c33dacfa1","annotations":[{"type":"blood_vessel","coordinates":[[[304,305],[303,305],[302,305],[301,305],[300,305],[299,305],[298,305],[297,305],[296,305],[295
{"id":"019390572feb","annotations":[{"type":"blood_vessel","coordinates":[[[107,357],[106,357],[105,357],[104,357],[104,356],[103,356],[102,356],[101,356],[100,356],[100
{"id":"01a7fca6263b","annotations":[{"type":"blood_vessel","coordinates":[[[85,136],[84,136],[83,136],[83,135],[82,135],[82,134],[82,133],[81,133],[80,133],[79,133],[78,
```


Figure 2: Image generation of mask and overlapping image

Here id represents the unique id assigned to the image. These annotations include the coordinates characterizing the region inside the picture as well as the kind of structure (e.g., glomerulus, blood artery).

To build masks matching to various annotation kinds, such as blood vessels and glomeruli, a specific function called create_mask is used. This method creates a unique masks for each type of annotation by filling polygons in a binary mask with ones using the OpenCV library. Masks are made for every annotated image when the images are loaded. The script makes sure the shapes of the pictures match and doesn't run files that aren't the right size. Masks are maintained in a nested dictionary (masks), sorted by picture ID and annotation type, whilst image data is arranged in a dictionary (images).

The display_image_and_masks function is called once a few sample image IDs are chosen in order to show how original photos and the annotations that go with them are shown visually. This step provides an actual example of how the method processes and displays the annotated medical images.

The images generated with mask and the overlapping image is shown below in Figure 3

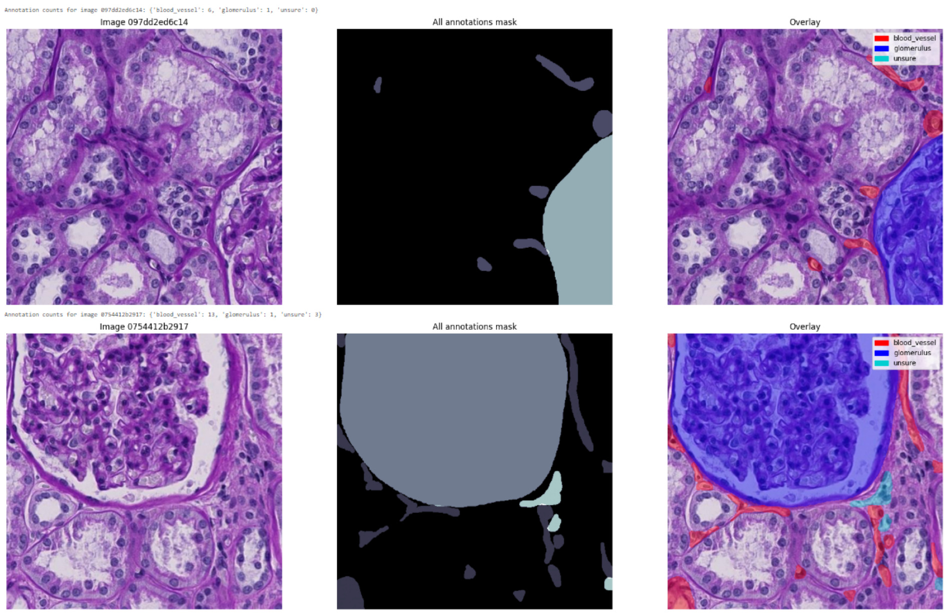

Figure 3: Image generation of mask and overlapping image

This methodical approach guarantees efficient loading of the data, annotation processing, and presentation of medical pictures, providing insightful information about the location and properties of vasculature in human tissues.

4.2 Data Preprocessing

The procedures for loading, preprocessing, and augmenting a dataset of medical pictures in order to train a machine learning model are described in this section of the approach. Every step is selected with care to improve the dataset's resilience and variety for efficient model training.

The function to load file paths based on a directory and a list of examples is defined at the start of the script. The goal of this phase is to create a list of file paths for the loading and processing of following images. To divide the file paths into training and validation sets, a function is implemented. Making sure the model is trained on a variety of photos while having a different set for assessment requires doing this crucial step. Because the split size is adjustable, it offers flexibility according to the size and properties of the dataset. Training and validation sets must be kept apart in order to evaluate model performance on unseen data. It makes it easy to avoid overfitting and ensures that the model can perform better on new data. A popular approach is an 80-20 split, which maintains a balance between the necessity of a sizable training period and a strong assessment phase.

There are defined functions for loading photos and matching masks. OpenCV is used to import the images, which are then transformed to float32 and normalized to a range between 0 and 1. Blood vessel-focused annotations from a JSON file are used to construct masks. This stage makes sure that the masks and pictures are ready for the next model training. In image processing, normalizing pixel values to a range between 0 and 1 is a standard procedure. It accelerates and balances the training process, which aids in the development of the model.

Using the supplied pictures and masks, a mapping function is constructed to transform the file paths into TensorFlow datasets. This function preprocesses the pictures and masks using TensorFlow's tf.numpy_function, adjusting their forms to ensure uniformity throughout the dataset.

In order to improve the generalization of the model and increase the variety of the dataset, data augmentation strategies are used. Images and masks are subjected to techniques like random flips and rotations. An additional approach for adding diversity to the dataset is the mosaic augmentation technique, which combines .four randomly selected images to form a mosaic. To improve the training dataset's variety, data augmentation is necessary. By randomly flipping and rotating, the model may be trained to learn invariant properties by simulating various vascular orientations. By combining many images, mosaic augmentation enhances the dataset with complex structures and patterns.

The dataset function receives the file locations and creates a TensorFlow dataset. It integrates the mapping function and, if provided, makes use of data augmentation techniques. The dataset is then batched for memory management, computational efficiency and improving the time it takes to train the data. During training, effective and parallelized data loading is ensured by using TensorFlow datasets.The mapping function makes it easier to translate file paths to image-mask pairs, providing straightforward interaction with the TensorFlow framework. Batching is a common technique to make sure maximum memory utilization takes place and computational effectiveness. It helps the model to improve convergence and stability during training by allowing it to adjust its weights based on many instances in each iteration. Eight has been selected as the batch size to balance model learning and computing efficiency.

Following the methodology, produces a well-structured and diversified dataset that can be used to train a machine learning model to precisely separate blood vessels in medical photographs. TensorFlow dataset features along with data augmentation approaches guarantee the effective and efficient use of the dataset for model training.

4.3 Model Development

Exponential Decay Learning Rate and Early Stopping are employed for both the model.

During training, the learning rate is dynamically adjusted using an exponential decay learning rate schedule. This ensures that the model will converge smoothly and gradually reduces the learning rate during training to prevent oscillations or overshooting during optimization.

One useful regularization strategy to avoid overfitting is early stopping. When the model begins to overfit the training data, the training process is stopped by keeping an eye on the validation loss. Maintaining optimal performance of the model on the validation set is ensured by restoring the best weights.

4.3.1 DeepLabV3+

The creation of the DeepLabV3+ model for the segmentation of the vasculature in medical pictures will be examined in this section of the implementation. It involves developing the training model, setting the parameters for the model, and creating the model architecture.

The model architecture uses a ResNet50 backbone for feature extraction and follows to the DeepLabV3+ concept. A Dilated Spatial Pyramid Pooling (DSPP) module in the design collects multi-scale contextual data. To improve the model's capacity to identify and divide up vascular structures of different sizes in medical pictures, the DSPP module is added. The DeepLabV3+ architecture is chosen due to its effectiveness in medical image segmentation task, namely in dilated convolutions for contextual information capture. Understanding this is crucial for identifying the many sized and contextual variations of vascular structures in medical imaging.

Because the ResNet50 backbone has a track record of successfully extracting hierarchical features from pictures, it is utilized for feature extraction. Conv4_block6_2_relu and conv2_block3_2_relu are the particular layers that were picked for the feature extraction; they were chosen with care to balance the trade-off between receptive field and spatial resolution.

For the purpose of obtaining contextual information at various scales without compromising spatial resolution, the DSPP module is essential. Applying varying rates of dilated convolutions enhances the model's chances to recognize various sized vascular structures. The model's comprehension of intricate spatial connections within the pictures is improved by the DSPP module.

When classifying each pixel as either vasculature or non-vasculature is the aim of binary segmentation tasks,Dice Loss coefficient is selected as the major loss function. Additionally, segmentation accuracy and the model's capacity to collect small features are enhanced by the inclusion of dice loss as a loss metric.

A statistic that improves segmentation efficiency is dice loss, especially when gathering small features. Binary Crossentropy is appropriate for binary segmentation tasks. Combining these two techniques gives us a better approach which will help us optimize our segementaion model.

Because features essential to vascular segmentation in medical pictures may differ considerably from features learnt on general-purpose image datasets, the ResNet50 backbone was designed without pre-trained weights. By training with random weights, the model can better adjust to the unique properties of the collection of images.

4.3.2 U-Net

The next step in the implementation is to create and train a U-Net model for the purpose of segmenting the vasculature in medical pictures. To retain spatial information, the encoder-decoder structure of the U-Net design has skip connections. A particular loss function, training metrics, and optimization technique are included in the model's compilation.

The U-Net architecture is selected due to its efficiency in tasks involving the segmentation of medical images. It is made up of a decoder that reconstructs the segmentation mask and an encoder that records hierarchical characteristics. The vanishing gradient issue is lessened and spatial features are preserved thanks to skip connections between matching encoder and decoder blocks.

The U-Net model's fundamental building components are convolutional blocks. Two convolutional layers make up each block, which are each followed by rectified linear unit (ReLU) activation and batch normalization. This combination gives the model non-linearity and helps in capturing minute details.

To increase the number of feature channels while downsampling the input image's spatial resolution, encoder blocks are employed. Max-pooling layers and convolutional blocks are examples of these blocks.Max-pooling reduces the spatial dimensions so that the model may focus on higher-level properties.

Upsampling the feature maps and recovering the segmentation mask's spatial information are the responsibilities of the decoder blocks. Upsampling is accomplished using transposed convolutional layers, and spatial information is preserved by concatenating skip connections from related encoder blocks.

Due to its effectiveness in adjusting the learning rate during training, the Adam optimizer was selected. It combines the benefits of momentum and adaptive learning rate techniques to provide faster convergence and better optimization.

The design decisions, optimization approach, and loss function are in line with industry best practices and are intended to provide reliable and accurate vascular segmentation.

4.4 Post Processing

Predictions for the validation dataset are produced using the trained segmentation model. To improve and fine-tune the anticipated masks, post-processing functions are created. In particular, dilation is done with a certain kernel and number of iterations to the anticipated masks. Dilation aids in filling in tiny gaps and softening the edges of the divided areas. With the compose function, a composite function is defined. This function enables the sequential application of many processing algorithms in a chain on the predictions.

The model's predictions are subjected to the composite function. This stage makes it possible to combine and apply flexible post-processing techniques, such dilatation, to the predictions.

To assess the effectiveness of the model's predictions quantitatively, the dice coefficient is computed. By comparing the anticipated and ground truth masks, the Dice coefficient calculates a similarity score between 0 and 1, with larger values denoting better segmentation accuracy.

For qualitative evaluation, the ground truth masks, original pictures, and forecasts are shown. The ground truth mask, the actual picture, and the anticipated mask make up each row in the display. The segmentation performance statistic is represented by the Dice coefficient.

5 Evaluation

Two models namely DeeplabV3plus and U-Net have been used for the task of image segmentation. The evaluation consists the architecture of the models, configurations set for the training and suitability of the models for the task of image segmentation.

DeeplabV3plus makes use of dilated convolutions and on the other hand U-Net employs an encoder-decoder structure paired with skip connections, these two models build are more than capable and are well-suited for capturing small details which is important for the task of medical image segmentation.

The models are optimized for precise blood vessel segmentation with the help of the Dice loss function. This approach corresponds to the high requirements of medical picture segmentation, where the accuracy of the segmentation is largely dependent on spatial overlap.

The models are set up with a dynamic learning rate schedule based on exponential decay and the Adam optimizer for best training results. In order to avoid overfitting and guarantee that the models perform effectively on unobserved medical pictures, early stopping is implemented. There is only 1 image present in the testing set, as it was the only image provided by the publisher of dataset.

5.1 Evaluation - DeeplabV3+

The architecture of DeeplabV3+ is selected because to its proficiency in medical picture segmentation. By utilizing dilated convolutions, the model exhibits an improved receptive field, which enables it to effectively extract contextual information that is essential for distinguishing complex blood artery architectures.

The Dice coefficient was used to evaluate the segmentation accuracy of predictions made by the DeeplabV3+ model. The average Dice coefficient for the model is 0.52 ± 0.1.

Figure 4 shows the difference between training dice coeff and validation dice coeff.

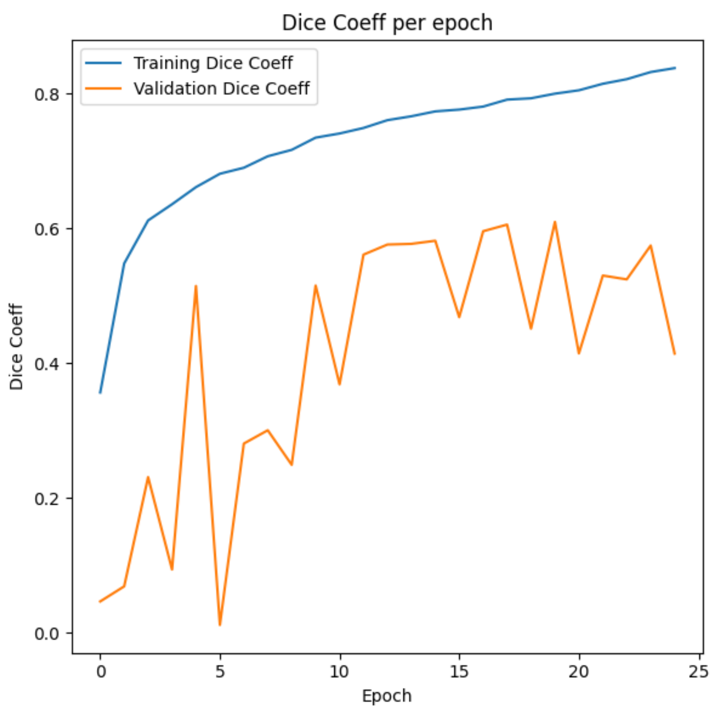

Figure 4: Image of Dice Coeff per epoch

Figure 5 shows the result generated by the model on the Test image of the dataset.

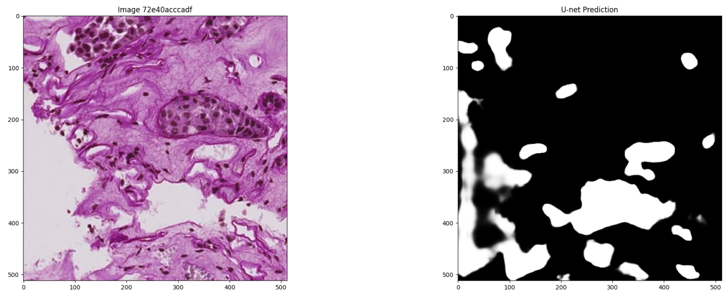

Figure 5: Image of result generated by the model on the Test image

Figure 6 shows the result generated by the model on validation set of the dataset.

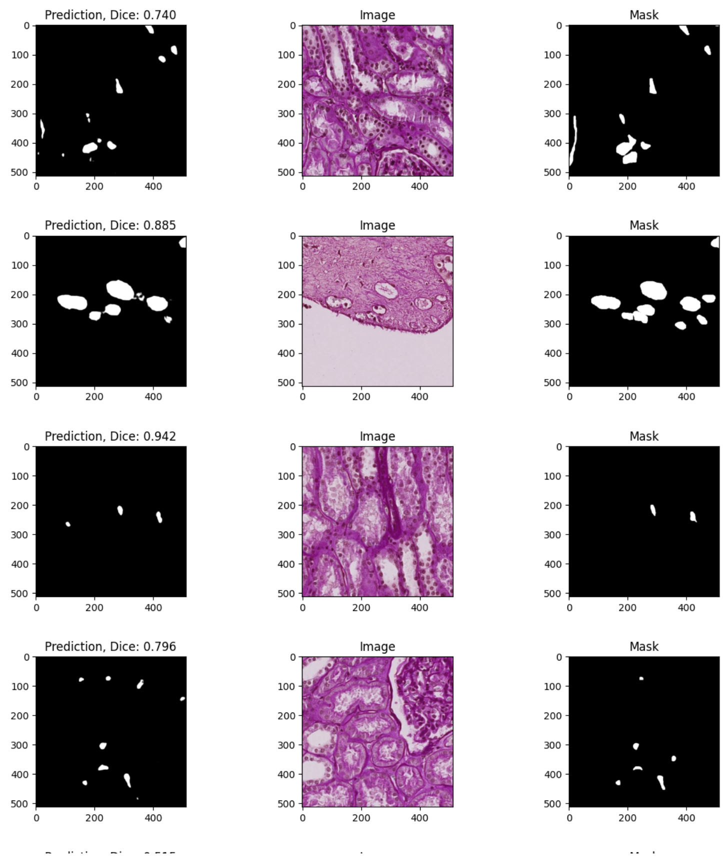

Figure 6: Image of result generated by the model on validation set

5.2 Evaluation - U-Net

U-Net's architecture is encoder-decoder. The decoder uses transposed convolutions to achieve exact localization, while the encoder records the image's context
The Dice coefficient was used to evaluate the segmentation accuracy of predictions made by the U-Net model. The average Dice coefficient for the model is 0.68 ± 0.1.

Figure 7 shows the difference between training dice coeff and validation dice coeff.

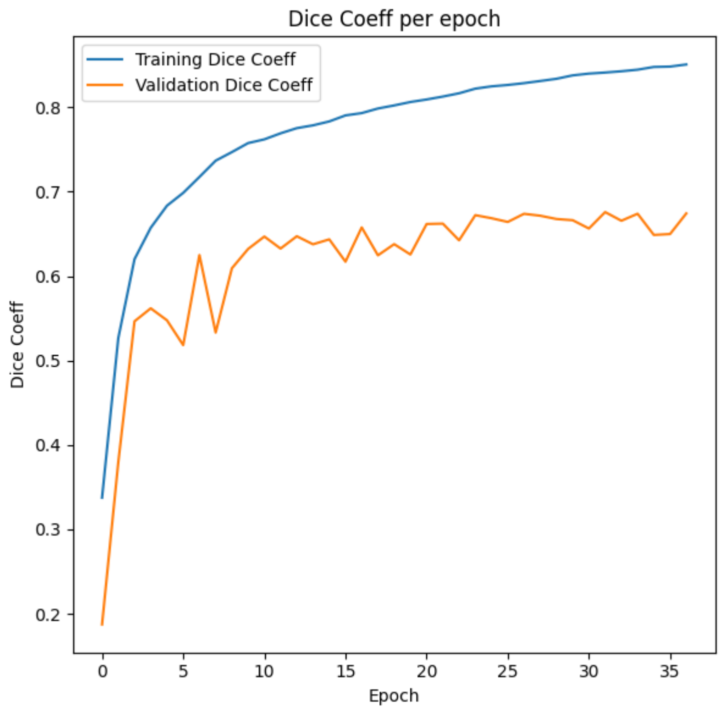

Figure 7: Image of Dice Coeff per epoch

Figure 8 shows the result generated by the model on the Test image of the dataset.

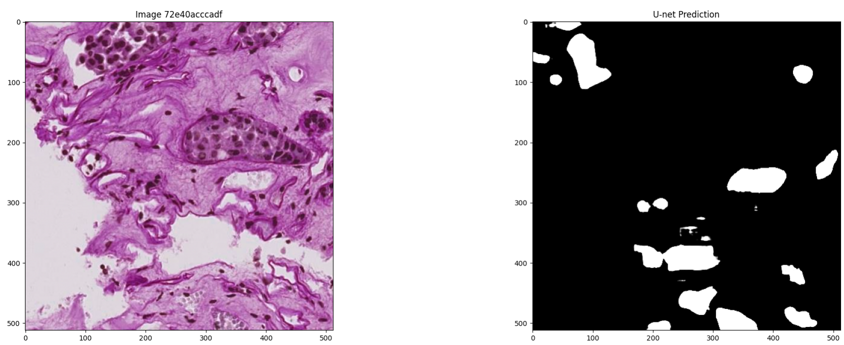

Figure 8: Image of result generated by the model on the Test image

Figure 9 shows the result generated by the model on validation set of the dataset.

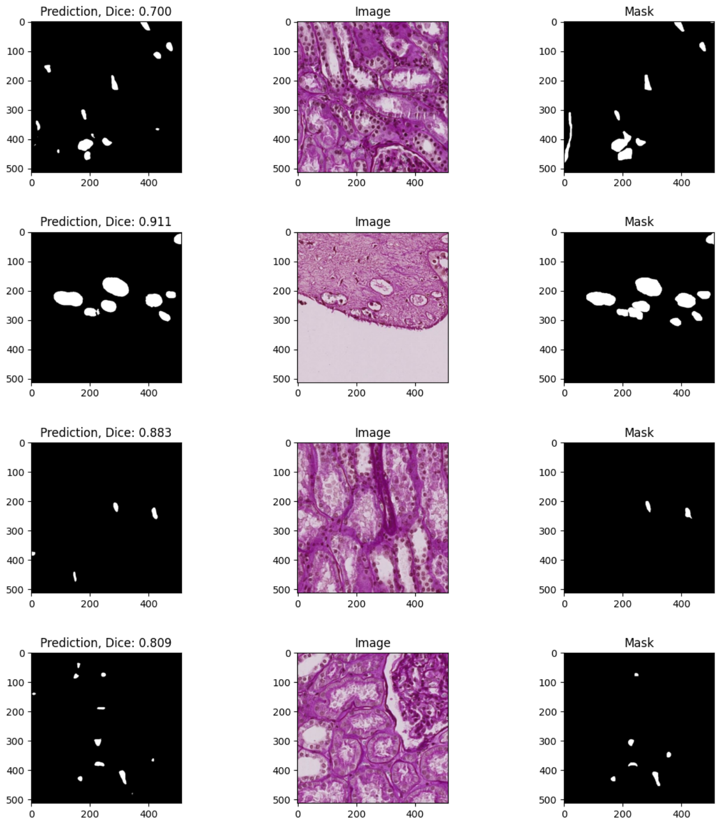

Figure 9: Image of result generated by the model on validation set

5.3 Discussion

In this discussion the performance of both the models will be addressed, both of the models have different architecture and different way of segmenting the image.

The U-Net's model has a symmetrical architecture, which combines a decoder for accurate localization and an encoder for contextual comprehension, is good at preserving spatial information—a crucial component in intricate segmentations like those needed for medical imaging. One noteworthy element that ensures little loss of data during the segmentation process is the introduction of skip links, which carry information straight from the encoder to the decoder.In the findings of the research, the design gets a good Dice coefficient of 0.68 ± 0.1, that shows the effectiveness in the medical segmentation task .

With a ResNet-based backbone, DeeplabV3+ integrates Atrous Spatial Pyramid Pooling (ASPP) into a more intricate structure. The ability to handle multi-scale data is a need for segmenting the features into various sizes in this design. With an average Dice coefficient of 0.52 ± 0.1, DeeplabV3+'s performance in this particular segmentation test was not as good as U-Net's, even with its improved capabilities. This could be because DeeplabV3+'s method isn't entirely consistent with the dataset's properties.

Both the models have many pros to them but there are some drawbacks in the model present. Although useful for some segmentation tasks, U-Net's relatively simplistic architecture might not be able to handle more intricate, high-level feature extractions. To increase its performance in more diverse and difficult datasets, improvements like the integration of deeper or more complex layers should be investigated. The Dice coefficient of the DeeplabV3+'s model indicates potential for improvement. Although a strength, the model's complexity may also be a disadvantage, creating difficulties for training and optimization. Its training effectiveness and generalization potential may also be enhanced by adding more sophisticated regularization algorithms and dynamic learning rate changes.

6 Conclusion and Future Work

In addressing the research question of what are the most effective way for segmentation of blood vessels in a health human tissue using machine learning model the study came to an conclusion that while leveraging deep learning and making use of different CNN's it was evident that utilizing U-Net is the effective way for this dataset. The results showed that U-Net was a better model compared to DeeplabV3+ as it had a better dice coefficient score, DeeplabV3+'s architecture and design didn't perform well on the Hupmap dataset, the dataset may have limited the model's effectiveness.
This research offers significant views on the selection and application of deep learning models in medical picture segmentation. It makes a point on how a selection of model's architecture is crucial with demands of image segmentation especially in the field of medical. The better performance by U-Net makes a point on how it has the potential to be dependable when it comes to tools related to treatment.

6.1 Future Work

6.1.1 Hybrid Model developmet

Hybrid model development involves combining the capabilities of DeeplabV3+ and U-Net to produce a model that is more accurate and efficient at handling a wider variety of medical imaging jobs.

6.1.2 Testing and Real-World Application

These models will be put into practice in actual clinical settings to assess their applicability and user-friendliness in a medical scenario.

6.1.3 Use of tranfer learning

looking at the use of transfer learning to modify these models for a larger range of medical imaging datasets, such as datasets with abnormalities or uncommon diseases.

6.1.4 Multi Class Clasification

As there are other elements present in the images in the dataset in future a model can be made that can classify the glomerulus present in the dataset currently the images that have glomerulus present in them are less in number.

6.1.5 Real world testing

The models can be test in real world clinical environment, so that we can get a clear outline on their real world applications and user friendliness.

References

Abdani, S. R., Zulkifley, M. A. and Moubark, A. M. (2020). Pterygium tissues segmentation using densely connected deeplab, *2020 IEEE 10th symposium on computer applications & industrial electronics (ISCAIE)*, IEEE, pp. 229–232.

Alsenan, A., Youssef, B. B. and Alhichri, H. (2021). A deep learning model based on mobilenetv3 and unet for spinal cord gray matter segmentation, *2021 44th International Conference on Telecommunications and Signal Processing (TSP)*, IEEE, pp. 244–248.

Azad, R., Heidari, M., Shariatnia, M., Aghdam, E. K., Karimijafarbigloo, S., Adeli, E. and Merhof, D. (2022). Transdeeplab: Convolution-free transformer-based deeplab v3+ for medical image segmentation, *International Workshop on PRedictive Intelligence In MEdicine*, Springer, pp. 91–102.

Chahal, E. S., Haritosh, A., Gupta, A., Gupta, K. and Sinha, A. (2019). Deep learning model for brain tumor segmentation & analysis, *2019 3rd International conference on recent developments in control, automation & power engineering (RDCAPE)*, IEEE, pp. 378–383.

Chen, K.-b., Xuan, Y., Lin, A.-j. and Guo, S.-h. (2021). Lung computed tomography image segmentation based on u-net network fused with dilated convolution, *Computer Methods and Programs in Biomedicine* **207**: 106170.

Groves, L. A., VanBerlo, B., Veinberg, N., Alboog, A., Peters, T. M. and Chen, E. C. (2020). Automatic segmentation of the carotid artery and internal jugular vein from 2d ultrasound images for 3d vascular reconstruction, *International journal of computer assisted radiology and surgery* **15**: 1835–1846.

Huang, H., Lin, L., Tong, R., Hu, H., Zhang, Q., Iwamoto, Y., Han, X., Chen, Y.-W. and Wu, J. (2020). Unet 3+: A full-scale connected unet for medical image segmentation, *ICASSP 2020-2020 IEEE international conference on acoustics, speech and signal processing (ICASSP)*, IEEE, pp. 1055–1059.

Jahnavi, T. and Vasundhara, D. (2022). Segmentation of medical images using u-net++, *2022 4th International Conference on Advances in Computing, Communication Control and Networking (ICAC3N)*, IEEE, pp. 801–807.

Jeong, J., Lei, Y., Kahn, S., Liu, T., Curran, W. J., Shu, H.-K., Mao, H. and Yang, X. (2020). Brain tumor segmentation using 3d mask r-cnn for dynamic susceptibility contrast enhanced perfusion imaging, *Physics in Medicine & Biology* **65**(18): 185009.

Kemnitz, J., Baumgartner, C. F., Eckstein, F., Chaudhari, A., Ruhdorfer, A., Wirth, W., Eder, S. K. and Konukoglu, E. (2020). Clinical evaluation of fully automated thigh muscle and adipose tissue segmentation using a u-net deep learning architecture in context of osteoarthritic knee pain, *Magnetic Resonance Materials in Physics, Biology and Medicine* **33**: 483–493.

Lenchik, L., Heacock, L., Weaver, A. A., Boutin, R. D., Cook, T. S., Itri, J., Filippi, C. G., Gullapalli, R. P., Lee, J., Zagurovskaya, M. et al. (2019). Automated segmentation of tissues using ct and mri: a systematic review, *Academic radiology* **26**(12): 1695–1706.

Luke, G. P., Hoffer-Hawlik, K., Van Namen, A. C. and Shang, R. (2019). O-net: a convolutional neural network for quantitative photoacoustic image segmentation and oximetry, *arXiv preprint arXiv:1911.01935* .

Mittal, M., Goyal, L. M., Kaur, S., Kaur, I., Verma, A. and Hemanth, D. J. (2019). Deep learning based enhanced tumor segmentation approach for mr brain images, *Applied Soft Computing* **78**: 346–354.

Oskal, K. R., Risdal, M., Janssen, E. A., Undersrud, E. S. and Gulsrud, T. O. (2019). A u-net based approach to epidermal tissue segmentation in whole slide histopathological images, *SN Applied Sciences* **1**: 1–12.

Saeedizadeh, N., Minaee, S., Kafieh, R., Yazdani, S. and Sonka, M. (2021). Covid tv-unet: Segmenting covid-19 chest ct images using connectivity imposed unet, *Computer methods and programs in biomedicine update* **1**: 100007.

Singh, P. and Cirrone, J. (2022). A data-efficient deep learning framework for segmentation and classification of histopathology images, *European Conference on Computer Vision*, Springer, pp. 385–405.

Takahashi, K., Abe, K., Kubota, S. I., Fukatsu, N., Morishita, Y., Yoshimatsu, Y., Hirakawa, S., Kubota, Y., Watabe, T., Ehata, S. et al. (2022). An analysis modality for vascular structures combining tissue-clearing technology and topological data analysis, *Nature communications* **13**(1): 5239.

Tang, W., Zou, D., Yang, S., Shi, J., Dan, J. and Song, G. (2020). A two-stage approach for automatic liver segmentation with faster r-cnn and deeplab, *Neural Computing and Applications* **32**: 6769–6778.

Todorov, M. I., Paetzold, J. C., Schoppe, O., Tetteh, G., Efremov, V., Völgyi, K., Düring, M., Dichgans, M., Piraud, M., Menze, B. et al. (2019). Automated analysis of whole brain vasculature using machine learning, *BioRxiv* p. 613257.

Todorov, M. I., Paetzold, J. C., Schoppe, O., Tetteh, G., Shit, S., Efremov, V., Todorov-Völgyi, K., Düring, M., Dichgans, M., Piraud, M. et al. (2020). Machine learning analysis of whole mouse brain vasculature, *Nature methods* **17**(4): 442–449.

Wolny, A., Cerrone, L., Vijayan, A., Tofanelli, R., Barro, A. V., Louveaux, M., Wenzl, C., Strauss, S., Wilson-Sánchez, D., Lymbouridou, R. et al. (2020). Accurate and versatile 3d segmentation of plant tissues at cellular resolution, *Elife* **9**: e57613.

Wu, J., Zhang, Y. and Tang, X. (2019). Simultaneous tissue classification and lateral ventricle segmentation via a 2d u-net driven by a 3d fully convolutional neural network, *2019 41st Annual International Conference of the IEEE Engineering in Medicine and Biology Society (EMBC)*, IEEE, pp. 5928–5931.